Quantum Criticality in the Two-Dimensional Periodic Anderson Model

T. Schäfer,[1,2,3] A. A. Katanin,[4] M. Kitatani,[1] A. Toschi,[1] and K. Held[1]
[1]*Institute of Solid State Physics, TU Wien, 1040 Vienna, Austria*
[2]*Collège de France, 11 place Marcelin Berthelot, 75005 Paris, France*
[3]*CPHT, CNRS, École Polytechnique, IP Paris, F-91128 Palaiseau, France*
[4]*Institute of Metal Physics, Kovalevskaya str. 18, 620990 Ekaterinburg, Russia*

(Received 10 December 2018; revised manuscript received 10 April 2019; published 6 June 2019)

We study the phase diagram and quantum critical region of one of the fundamental models for electronic correlations: the periodic Anderson model. Employing the recently developed dynamical vertex approximation, we find a phase transition between a zero-temperature antiferromagnetic insulator and a Kondo insulator. In the quantum critical region, we determine a critical exponent $\gamma = 2$ for the antiferromagnetic susceptibility. At higher temperatures, we have free spins with $\gamma = 1$ instead, whereas at lower temperatures, there is an even stronger increase and suppression of the susceptibility below and above the quantum critical point, respectively.

DOI: 10.1103/PhysRevLett.122.227201

Introduction.—Quantum phase transitions are exceedingly exciting since, besides the spatial correlations of a classical phase transition, also (quantum) correlations in time become relevant at zero temperature T. This changes the universality class, i.e., the critical exponents, and can be best understood when considering imaginary time τ which is restricted to $\tau \in [0, 1/T]$. Hence, at any finite T, temporal (quantum) correlations are cut off at $1/T$ so that only the spatial correlations remain relevant [1].

On the experimental side, the most well studied are quantum critical points (QCPs) in heavy fermion systems [2,3] such as $CeCu_{6-x}Au_x$ [4] and $YbRh_2Si_2$ [5,6]. Experimentally accessible is the unusual behavior within the quantum critical region at a finite T above the QCP; for a schematic, see Fig. 1. The theoretical description of such heavy fermion QCPs is, however, still in its infancy.

The conventional Hertz[7]-Moriya[8]-Millis[9] (HMM) theory relies on the consideration of the effective ϕ^4 model for magnetic degrees of freedom and may hence not be applicable for heavy fermion systems with their strong electronic correlations. HMM theory is by construction a (renormalized) weak-coupling approach which is also valid above the upper critical dimension, i.e., for $d_{\text{eff}} = d + z > 4$. Here, the spatial dimensions d need to be supplemented by a dynamical exponent z, which relates the critical behavior of the correlation length in space ($\xi \sim T^{-\nu}$; ν: critical exponent) and time ($\xi_\tau \sim T^{-z\nu}$) at the QCP. Other proposals for a solution of the antiferromagnetic (metallic) criticality problem include the fractionalized electron picture [10], the critical quasiparticle theory [11], and the strong coupling theory [12]; see also [13–17] for quantum criticality studies employing other methods.

Quantum criticality below the upper critical dimension for $d_{\text{eff}} = 3$ ($d = 2$, $z = 1$) was considered by Chubukov *et al.* [18] for the Heisenberg model within a $1/N$ expansion and by renormalization-group approaches for Ising symmetry [19,20]. But again, these approaches cannot be straightforwardly extended to include fermionic excitations, which are actually essential regarding the experimental realization of QCPs in heavy-fermion systems. Despite many promising approaches [1,2,21–24], we hitherto still lack a reliable solution even for the simplest model for heavy fermion QCPs, the periodic Anderson model (PAM) beyond a mere (conjectured) mapping onto bosonic models.

In this Letter, we hence analyze the QCP of the PAM by means of a recently developed method, the dynamical vertex approximation (DΓA) [25,26]. The DΓA is, similar as related approaches [27–31], a diagrammatic extension of the dynamical mean field theory (DMFT) [32–34]; for a recent review, see Ref. [35]. From the DMFT it inherits a

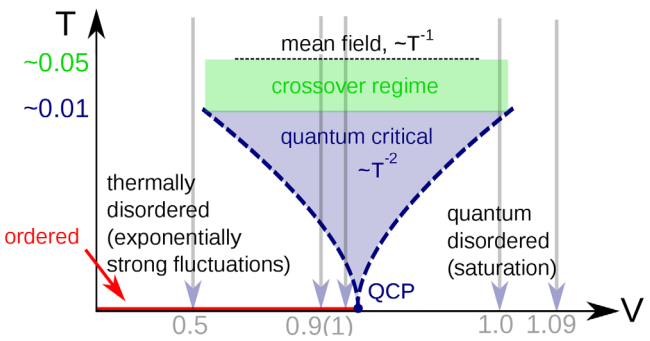

FIG. 1. Schematic phase diagram of the symmetric PAM with a $T = 0$ quantum phase transition toward an antiferromagnetic insulator in $d = 2$. Emanating from the QCP, is a quantum critical region with particular critical exponents. The parameters and values indicate actual DΓA results presented below.

reliable and nonperturbative description of (local) temporal correlations. But on top of these, also nonlocal spatial correlations are taken into account by means of ladder or parquet diagrams, which do not take the bare interaction but the local irreducible or fully irreducible vertex as a building block. These diagrammatic extensions have been successfully employed for studying critical exponents and phenomena in the Hubbard and Falicov-Kimball model [36–40]. We are hence in the fortunate situation that we can revisit quantum criticality in fermionic models thanks to recent methodological progress.

Model and analytical considerations.—To arrive at a non-mean-field, non-Gaussian critical behavior we study the PAM in $d = 2$ which can be expected to have the same quantum critical exponents as the Heisenberg model, which in turn has a conjectured $z = 1$ [18,41]. This suggests an effective dimension $d_{\text{eff}} = 2 + 1 = 3$ [42]. The Hamiltonian of the PAM reads

$$\mathcal{H} = \sum_{\mathbf{k},\sigma} \varepsilon_{\mathbf{k}} d^{\dagger}_{\mathbf{k}\sigma} d_{\mathbf{k}\sigma} + \varepsilon_f \sum_{i\sigma} f^{\dagger}_{i\sigma} f_{i\sigma} + U \sum_i n_{f,i\uparrow} n_{f,i\downarrow} + V \sum_{i,\sigma} [d^{\dagger}_{i\sigma} f_{i\sigma} + f^{\dagger}_{i\sigma} d_{i\sigma}]. \quad (1)$$

It consists of localized f electrons with creation (annihilation) operators $f^{\dagger}_{i\sigma}$ ($f_{i\sigma}$), $n_{f,i\sigma} = f^{\dagger}_{i\sigma} f_{i\sigma}$, interacting through a local Coulomb repulsion U and with a local one-particle potential ε_f. Further, there are itinerant $d^{\dagger}_{i\sigma}$ ($d_{i\sigma}$) electrons with a nearest neighbor hopping t, or a corresponding energy-momentum dispersion relation $\varepsilon_{\mathbf{k}} = -2t[\cos(k_x) + \cos(k_y)]$. Finally, there is a hybridization V between both kinds of electrons. In the presented calculations, we fix $U = 4t$ (intermediate-to-strong coupling). We consider the half-filled case $\varepsilon_f = -U/2$, for which the PAM maps onto the Kondo lattice model with a coupling $J = 8V^2/U$ in the limit $U \gg V$. That is, for large U, the f electrons form localized spins. This Kondo lattice model shows the famous Doniach [43] T-V phase diagram, with two competing phases.

On the one hand, there is the Kondo effect [44]: the spins, that are free at high T with a Curie susceptibility $\chi \sim T^{-1}$ get screened below the Kondo temperature T_K. In this case, a Kondo resonance forms at the Fermi level. In our particle-hole symmetric case of half filling, this Kondo resonance is however gapped. This can be understood starting from the noninteracting model ($U = 0$): the flat f band at the Fermi energy E_F hybridizes with the dispersive conduction d band so that a hybridization gap opens at E_F. That is, we have a band insulator and for a finite U a quasiparticle-(Kondo-)renormalized picture thereof, i.e., a Kondo insulator. For the (single-site) Kondo model

$$T_K \sim e^{-(1/\rho_0 J)}, \quad (2)$$

where ρ_0 is the noninteracting density of states of the conduction electrons at the Fermi level [44,45]. For the PAM we get a similar, somewhat enhanced T_K [45,52].

Competing with the Kondo effect is a magnetic phase, which can be understood as the effective Ruderman-Kittel-Kasuya-Yosida (RKKY) coupling between f-electron spins through the conduction electrons. In second order perturbation theory in J, the coupling strength and hence the critical temperature is

$$T_{\text{RKKY}} = \frac{1}{4} J^2 \chi^{\omega=0}_{0,\mathbf{Q}}, \quad (3)$$

where χ_0 is the (noninteracting; $V = 0$) susceptibility of the conduction electrons and the factor $1/4 = S(S+1)/3$ for spin $S = 1/2$ corresponds to the mean-field critical temperature. In our case, the maximal coupling appears at the antiferromagnetic (AF) wave vector $\mathbf{Q} = (\pi, \pi)$. An AF ordering opens a gap, so that we obtain an AF insulator. Since T_K is exponentially small for small J [43], T_{RKKY} prevails for small J, whereas at large J the Kondo effect wins. Hence, there is a phase transition from an AF to a Kondo insulator at $T_K \approx T_{\text{RKKY}}$. Hence, the ground state is always insulating. At high temperatures, the f electrons are also gapped and form free spins, but the conducting electrons are itinerant; at $T \gtrsim T_K$ the Kondo peak starts to develop but the Kondo insulating gap that is present at lower Ts is still smeared out due to strong scattering.

Phase diagram.—Figure 2 presents the actual phase diagram of the PAM as calculated using DMFT and DΓA. Here, we employ the ladder DΓA with Moriya-λ correction [53] which generates spin fluctuations starting from the local vertex Γ calculated for a converged DMFT solution; for further details on the method, we refer the reader to Refs. [35,54–57]. For the DMFT phase diagram of the

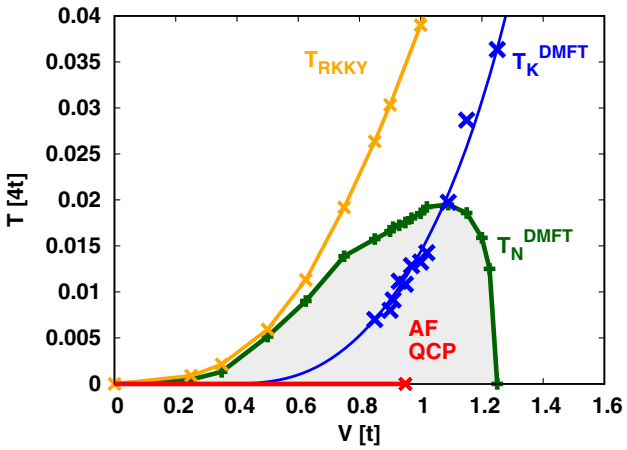

FIG. 2. Phase diagram T vs V of the half-filled $2d$ PAM at $U = 4t$. The figure shows the AF transition T_N line in DMFT (green) and DΓA (red), the DMFT Kondo-temperature $T_{\text{K}}^{\text{DMFT}}$ (blue), and T_{RKKY} [yellow, calculated from Eq. (3), cf. Ref. [7] of the Supplemental Material [45]].

Kondo lattice model (and including short-ranged correlations), cf. Refs. [58–60].

Let us start with the DMFT results, which show AF order at small V in the light-green shaded region of Fig. 2. This order breaks down as the Kondo effect sets in and a QCP emerges: there is a $T = 0$ phase transition. As we see, the perturbative result, $T_{\mathrm{RKKY}} \sim J^2 \sim V^4$ (yellow line), only holds for small V; for larger Vs DMFT yields a smaller AF transition temperature due to temporal correlations (green line). As we see the AF order breaks down when the DMFT Kondo temperature (blue line, determined from the maximum of the local susceptibility as a function of T) becomes of similar amplitude as the DMFT Néel temperature (green line).

The DΓA phase diagram in Fig. 2 is distinctively different. Concomitant with the Mermin-Wagner theorem [61], AF order is only found at $T = 0$ because of strong nonlocal fluctuations in $d = 2$, cf. Ref. [26] for DΓA fulfilling the Mermin-Wagner theorem for the $2d$ Hubbard model. Nonetheless, we have AF order along the red line in Figs. 1 and 2, and hence, at $T = 0$, a QCP develops at $V_{\mathrm{QCP}} \approx 0.91t$.

Quantum critical region.—Above this QCP region we expect a quantum critical region as visualized in Fig. 1, with non-Gaussian fluctuations. Hence, we study the AF susceptibility $\chi = \chi_{\mathbf{Q}}^{\omega=0}$ at momentum $\mathbf{Q} = (\pi, \pi)$ and its critical behavior around the critical V_{QCP} in Fig. 3. In DMFT, $\chi \sim (T - T_N)^{-\gamma} \sim (T - T_N)^{-1}$; see Fig. 3 (upper panels) so that we have a critical exponent $\gamma = 1$. This reflects the (bosonic) mean-field critical behavior of DMFT which neglects spatial fluctuations. At high temperatures, it smoothly evolves into the Curie susceptibility $\chi \sim T^{-1}$ of free spins.

In DΓA, Fig. 3 (lower panels), we observe a completely different behavior. While at high T, we have the same $\gamma = 1$ Curie behavior, there is a crossover to $\chi \sim T^{-2}$, i.e., a quantum critical exponent $\gamma = 2$ at lower Ts. This critical exponent and the related correlation length $\xi \sim T^{-\nu} \sim T^{-1}$ agree with the conjectured mapping onto a nonlinear σ model [18,62], which also displays antiferromagnetic ordering within an insulating phase (as we have) with a dynamical critical exponent $z = 1$ and yields the same $\xi \sim 1/T$ in the quantum critical regime. This yields the critical exponent $\nu = 1$ for the correlation length, which happens to be the same critical exponent that one gets if setting the correlation length in time to its cutoff $\xi_\tau \sim 1/T$ and accepting that $z = 1$. With the Fisher relation $\gamma/\nu = 2 - \eta$ [63], $\gamma \approx 2$ for the susceptibility as observed in Fig. 3 (note that, typically, η is vanishingly small even in $d = 2$). In the Supplemental Material, Sec. S3 [45], we present an explanation for this critical exponent on the basis of a sum rule .

With increasing dimensionality, we expect the critical exponents at $d \geq 3$ approach their values in HMM theory [45]. Computing quantum critical exponents of strongly correlated electron models such as the PAM was, however, not possible hitherto; quantum Monte Carlo simulations and cluster extensions of DMFT are restricted to too short-ranged correlations.

At the lowest T, deviations from this quantum critical behavior are discernible in Fig. 3 (lower panels) and are to be expected as we leave the cone-shaped quantum critical region in Fig. 1. For $V < V_{\mathrm{QCP}}$, eventually antiferromagnetic order sets in at $T = 0$. Already at finite Ts, an exponential increase of the correlation length and the susceptibility with $1/T$ is to be expected [62]. A similar exponential scaling was observed for the Hubbard model [64]. Consistently with this description, one observes a deviation to even larger susceptibilities at $V \ll V_{\mathrm{QCP}}$ and lowest Ts in Fig. 3. For low T and $V > V_{\mathrm{QCP}}$, on the other hand, eventually a Kondo insulating phase develops (quantum disordered phase in Fig. 1). For this (renormalized) band insulator, one has $\chi \to 0$ for $T \to 0$. In agreement with this, Fig. 3 shows a deviation to smaller

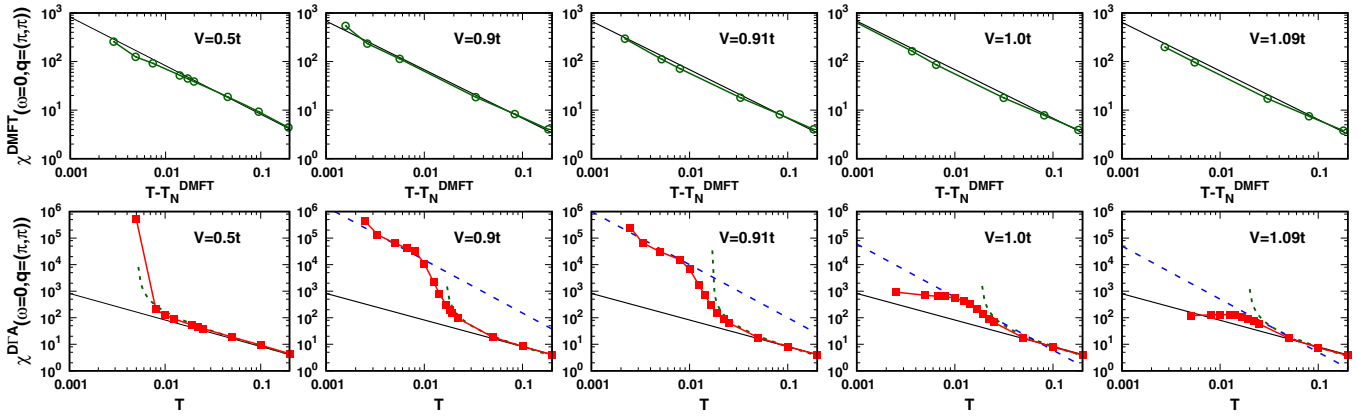

FIG. 3. Magnetic susceptibilities (on a double logarithmic scale) in DMFT (upper panel, dark green open circles) and DΓA (lower panel, red squares). The black solid and blue dotted lines indicate a $\chi \sim T^{-1}$ and $\chi \sim T^{-2}$ behavior, respectively; the green dashed line is the DMFT susceptibility $\chi \sim (T - T_{\mathrm{DMFT}})^{-1}$ (black line from the upper panel).

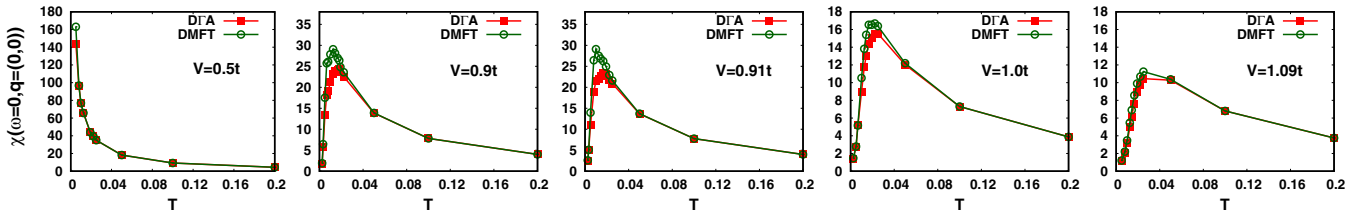

FIG. 4. Ferromagnetic susceptibility in DMFT (dark green open circles) and DΓA (red squares) for the same parameters as in Fig. 3.

susceptibilities at lower Ts; a full suppression of the susceptibility because of the Kondo gap will only occur at larger V in the accessible T range.

An intriguing, nonuniversal aspect is the strong enhancement of the susceptibility in the crossover regime between the $\chi \sim 1/T$ and $\chi \sim 1/T^2$ behavior, in particular at $V = 0.9$ and $V = 0.91$ in Fig. 3. This originates from enhanced antiferromagnetic correlations, which for the periodic Anderson model set in somewhat above T_{DMFT} (see green line in Fig. 3) and then crossover to the quantum critical $\chi \sim 1/T^2$ region, however with a much larger quantum critical susceptibility (prefactor thereof) than for a Heisenberg model with the exchange interaction providing the same mean-field transition temperature. For a more detailed discussion, see the Supplemental Material, Sec. S.4 [45].

Altogether our results yield the quantum critical region schematically presented in Fig. 1, where we have also inserted the actual V values employed in our calculation, along with the observed exponents of the T dependence of the susceptibility.

Uniform susceptibility.—Let us now turn to the (uniform) susceptibility, i.e., $\chi^{\omega=0}_{\mathbf{Q}}$ at momentum $\mathbf{Q} = (0, 0)$, which has the advantage that it can be measured more directly in experiment. Its T dependence around V_{QCP} is displayed in Fig. 4. At large T it shows, similar as the antiferromagnetic χ, the $1/T$ Curie behavior of free spins. However, as the spins get screened through the Kondo effect, the ferromagnetic susceptibility shows a maximum around the T_K of Fig. 4, whereas the antiferromagnetic susceptibility in Fig. 3 further grows, signaling the instability toward AF. Below this maximum, the ferromagnetic susceptibility $\chi^{\omega=0}_{\mathbf{Q}=(0,0)}$ shows essentially in a T-linear behavior in the quantum critical region. Such a behavior has also been reported for a nonlinear σ model and $1/N$ calculations [18].

Conclusion.—Thanks to an advanced many-body method, the DΓA, we are finally able to study the phase diagram and even the quantum critical behavior of the PAM, the prime model for heavy fermions, in $d = 2$. We find antiferromagnetic order for small hybridizations $V < V_{\mathrm{QCP}}$ at $T = 0$, consistent with the Mermin-Wagner theorem in DΓA. In DMFT, antiferromagnetism breaks down when the Kondo temperature T_K exceeds the Néel temperature T_N, as in the Doniach scenario, giving rise to a QCP. While $T_N = 0$ in DΓA, we still get a comparable V_{QCP}, which is 25% smaller in DΓA than in DMFT as the latter neglects nonlocal spin fluctuations.

We identify a quantum critical region with critical exponents $\nu = 1$ for the correlation length and $\gamma = 2$ for the antiferromagnetic susceptibility, as displayed in Fig. 1, whereas the uniform susceptibility shows a noncritical linear-T dependence. Above the quantum critical region, we observe free spins with $\gamma = 1$ at high T, while at small T, the AF susceptibility is exponentially enhanced in the thermally disordered region $V < V_{\mathrm{QCP}}$ and suppressed in the quantum disordered, Kondo insulating region $V > V_{\mathrm{QCP}}$.

Our work opens a route for studying quantum criticality in various models, which was hitherto only possible for spin models but not for correlated electrons. This removes a blank spot on the map of quantum critical theories, which bear many sophisticated quantum field theoretical considerations, analytical arguments, and derivations, but few means to test these numerically in a reliable way.

We would like to thank Fakher Asaad and Patrick Chalupa for stimulating discussions. The present work was supported by the European Research Council under the European Union's Seventh Framework Program (FP7/2007–2013) through ERC Grant No. 306447, Spezialforschungsbereich Vienna Computational Materials Laboratory (M. K., T. S., K. H.), Austrian Science Fund (FWF) through the Doctoral School "Building Solids for Function" (T. S.), the Erwin-Schrödinger Fellowship J 4266 (SuMo, T. S.) and Project I 2794-N35 (A. T.), as well as the Russian Federation through theme "Quant" AAAA-A18-118020190095-4 of Minobrnauki of Russia (A. A. K.). T. S. further acknowledges the European Research Council for the European Union's Seventh Framework Program (FP7/2007–2013) with ERC Grant No. 319286 (QMAC) and received funding through the "Exzellenzstipendium Promotio sub auspiciis praesidentis rei publicae" of the Federal Ministry of Education, Science and Research of Austria. Calculations have been done mainly on the Vienna Scientific Cluster (VSC).

[1] S. Sachdev, *Quantum Phase Transitions* (Cambridge University Press, Cambridge, United Kingdom, 1999).
[2] H. v. Löhneysen, A. Rosch, M. Vojta, and P. Wölfle, Rev. Mod. Phys. **79**, 1015 (2007).

[3] M. Brando, D. Belitz, F. M. Grosche, and T. R. Kirkpatrick, Rev. Mod. Phys. **88**, 025006 (2016).
[4] A. Schröder, G. Aeppli, R. Coldea, M. Adams, O. Stockert, H. v. Löhneysen, E. Bucher, R. Ramazashvili, and P. Coleman, Nature (London) **407**, 351 (2000).
[5] J. Custers, P. Gegenwart, H. Wilhelm, K. Neumaier, Y. Tokiwa, O. Trovarelli, C. Geibl, F. Steglich, C. Pépin, and P. Coleman, Nature (London) **424**, 524 (2003).
[6] S. Paschen, T. Lühmann, S. Wirth, P. Gegenwart, O. Trovarelli, C. Geibl, F. Steglich, P. Coleman, and Q. Si, Nature (London) **432**, 881 (2004).
[7] J. A. Hertz, Phys. Rev. B **14**, 1165 (1976).
[8] T. Moriya and A. Kawabata, J. Phys. Soc. Jpn. **34**, 639 (1973).
[9] A. J. Millis, Phys. Rev. B **48**, 7183 (1993).
[10] S. Sachdev, Nat. Phys. **4**, 173 (2008).
[11] Special issue on Mottness, T. Senthil, Ann. Phys. (Amsterdam) **321**, 1669 (2006)].
[12] E. Abrahams, J. Schmalian, and P. Wölfle, Phys. Rev. B **90**, 045105 (2014).
[13] M. Vekić, J. W. Cannon, D. J. Scalapino, R. T. Scalettar, and R. L. Sugar, Phys. Rev. Lett. **74**, 2367 (1995).
[14] W. Hu, R. T. Scalettar, E. W. Huang, and B. Moritz, Phys. Rev. B **95**, 235122 (2017).
[15] H. Terletska, J. Vučičević, D. Tanasković, and V. Dobrosavljević, Phys. Rev. Lett. **107**, 026401 (2011).
[16] P. Haldar, M. S. Laad, and S. R. Hassan, Phys. Rev. B **94**, 081115(R) (2016).
[17] B. Lenz, S. R. Manmana, T. Pruschke, F. F. Assaad, and M. Raczkowski, Phys. Rev. Lett. **116**, 086403 (2016).
[18] A. V. Chubukov, S. Sachdev, and J. Ye, Phys. Rev. B **49**, 11919 (1994).
[19] S. Sachdev, Phys. Rev. B **55**, 142 (1997).
[20] P. Strack and P. Jakubczyk, Phys. Rev. B **80**, 085108 (2009).
[21] Q. Si, S. Rabello, K. Ingersent, and J. L. Smith, Nature (London) **413**, 804 (2001).
[22] P. Coleman, Nature (London) **433**, 226 (2005).
[23] A. Kopp and S. Chakravarty, Nat. Phys. **1**, 53 (2005).
[24] P. Strack, PhD thesis, University of Stuttgart, 2009, https://arxiv.org/abs/1109.1859.
[25] A. Toschi, A. A. Katanin, and K. Held, Phys. Rev. B **75**, 045118 (2007).
[26] A. A. Katanin, A. Toschi, and K. Held, Phys. Rev. B **80**, 075104 (2009).
[27] A. N. Rubtsov, M. I. Katsnelson, and A. I. Lichtenstein, Phys. Rev. B **77**, 033101 (2008).
[28] G. Rohringer, A. Toschi, H. Hafermann, K. Held, V. I. Anisimov, and A. A. Katanin, Phys. Rev. B **88**, 115112 (2013).
[29] C. Taranto, S. Andergassen, J. Bauer, K. Held, A. Katanin, W. Metzner, G. Rohringer, and A. Toschi, Phys. Rev. Lett. **112**, 196402 (2014).
[30] T. Ayral and O. Parcollet, Phys. Rev. B **92**, 115109 (2015).
[31] G. Li, Phys. Rev. B **91**, 165134 (2015).
[32] W. Metzner and D. Vollhardt, Phys. Rev. Lett. **62**, 324 (1989).
[33] A. Georges and G. Kotliar, Phys. Rev. B **45**, 6479 (1992).
[34] A. Georges, G. Kotliar, W. Krauth, and M. J. Rozenberg, Rev. Mod. Phys. **68**, 13 (1996).
[35] G. Rohringer, H. Hafermann, A. Toschi, A. A. Katanin, A. E. Antipov, M. I. Katsnelson, A. I. Lichtenstein, A. N. Rubtsov, and K. Held, Rev. Mod. Phys. **90**, 025003 (2018).
[36] G. Rohringer, A. Toschi, A. Katanin, and K. Held, Phys. Rev. Lett. **107**, 256402 (2011).
[37] T. Schäfer, A. A. Katanin, K. Held, and A. Toschi, Phys. Rev. Lett. **119**, 046402 (2017).
[38] A. E. Antipov, E. Gull, and S. Kirchner, Phys. Rev. Lett. **112**, 226401 (2014).
[39] D. Hirschmeier, H. Hafermann, E. Gull, A. I. Lichtenstein, and A. E. Antipov, Phys. Rev. B **92**, 144409 (2015).
[40] L. Del Re, M. Capone, and A. Toschi, Phys. Rev. B **99**, 045137 (2019).
[41] M. Troyer, M. Imada, and K. Ueda, J. Phys. Soc. Jpn. **66**, 2957 (1997).
[42] Note that in Ref. [37] the Hubbard model was studied for $d = 3$ which, together with the expected $z = 2$ for a metallic antiferromagnetic phase transition, would yield $d_{\text{eff}} = 5 > 4$. However, $\nu = 1$ instead of the HMM value $\nu = (d + z - 2)/(2z) = 3/4$ [2] was obtained, because of peculiarities of the Fermi surface, the so-called Kohn lines. This physics, however, can still be understood in terms of Gaussian fluctuations, e.g., in the random phase approximation [37].
[43] S. Doniach, Physica (Amsterdam) **91(B+C)**, 231 (1977).
[44] A. Hewson, *The Kondo Problem to Heavy Fermions* (Cambridge University Press, Cambridge, United Kingdom, 1993).
[45] See Supplemental Material at http://link.aps.org/supplemental/10.1103/PhysRevLett.122.227201, we add information on how we determine the DMFT T_K in Sec. S.1, the momentum grid convergence in Sec. S.2, analytic calculations for the quantum critical exponent in Sec. S.3, and a comparison to the Heisenberg susceptibility in Sec. S.4. The Supplemental Material includes Refs. [46–51].
[46] H. R. Krishna-murthy, J. W. Wilkins, and K. G. Wilson, Phys. Rev. B **21**, 1003 (1980).
[47] P. Chalupa, P. Gunacker, T. Schäfer, K. Held, and A. Toschi, Phys. Rev. B **97**, 245136 (2018).
[48] H. Kang, K. Haule, G. Kotliar, P. Coleman, and J.-H. Shim, Phys. Rev. B **99**, 165115 (2019).
[49] M. Kitatani, T. Schäfer, H. Aoki, and K. Held, Phys. Rev. B **99**, 041115(R) (2019).
[50] V. Y. Irkhin and A. A. Katanin, Phys. Rev. B **55**, 12318 (1997).
[51] V. Y. Irkhin, A. A. Katanin, and M. I. Katsnelson, Phys. Rev. B **60**, 1082 (1999).
[52] T. Pruschke, R. Bulla, and M. Jarrell, Phys. Rev. B **61**, 12799 (2000).
[53] G. Rohringer and A. Toschi, Phys. Rev. B **94**, 125144 (2016).
[54] G. Rohringer, A. Valli, and A. Toschi, Phys. Rev. B **86**, 125114 (2012).
[55] T. Schäfer, G. Rohringer, O. Gunnarsson, S. Ciuchi, G. Sangiovanni, and A. Toschi, Phys. Rev. Lett. **110**, 246405 (2013).

[56] N. Wentzell, G. Li, A. Tagliavini, C. Taranto, G. Rohringer, K. Held, A. Toschi, and S. Andergassen, arXiv: 1610.06520.
[57] J. Kaufmann, P. Gunacker, and K. Held, Phys. Rev. B **96**, 035114 (2017).
[58] J. Otsuki, H. Kusunose, and Y. Kuramoto, Phys. Rev. Lett. **102**, 017202 (2009).
[59] L. C. Martin, M. Bercx, and F. F. Assaad, Phys. Rev. B **82**, 245105 (2010).
[60] B. Lenz, R. Gezzi, and S. R. Manmana, Phys. Rev. B **96**, 155119 (2017).
[61] N. D. Mermin and H. Wagner, Phys. Rev. Lett. **17**, 1307 (1966).
[62] S. Chakravarty, B. I. Halperin, and D. R. Nelson, Phys. Rev. Lett. **60**, 1057 (1988).
[63] M. E. Fisher, Rep. Prog. Phys. **30**, 615 (1967).
[64] T. Schäfer, F. Geles, D. Rost, G. Rohringer, E. Arrigoni, K. Held, N. Blümer, M. Aichhorn, and A. Toschi, Phys. Rev. B **91**, 125109 (2015).